

## Design of the Prototype Negative Ion Source for Neutral Beam Injector at ASIPP

This content has been downloaded from IOPscience. Please scroll down to see the full text.

2016 Plasma Sci. Technol. 18 954

(<http://iopscience.iop.org/1009-0630/18/9/954>)

View [the table of contents for this issue](#), or go to the [journal homepage](#) for more

Download details:

IP Address: 211.86.158.36

This content was downloaded on 10/04/2017 at 03:27

Please note that [terms and conditions apply](#).

You may also be interested in:

[Development of Distributed Control System for Neutral Beam Injector on EAST](#)

Sheng Peng, Hu Chundong, Cui Qinglong et al.

[The Supervisory Control System for the HL-2A Neutral Beam Injector](#)

Li Bo, Li Li, Feng Kun et al.

[Recent Progress of Neutral Beam Injector and Beam Emission Diagnosis in LHD](#)

Katsunori Ikeda, Kenichi Nagaoka, Yasuhiko Takeiri et al.

[Development of a Data Acquisition Control System for the First NBI on EAST](#)

Zhang Xiaodan, Hu Chundong, Sheng Peng et al.

[First Achievement of Plasma Heating for EAST Neutral Beam Injector](#)

Hu Chundong and NBI team

[The Timing System of the Neutral Beam Injector on EAST](#)

Sheng Peng, Hu Chundong, Zhao Yuanzhe et al.

[Preliminary Results of Ion Beam Extraction Tests on EAST Neutral Beam Injector](#)

Hu Chundong

[3D modelling of negative ion extraction from a negative ion source](#)

S. Mochalsky, A.F. Lifschitz and T. Minea

[Numerical study of beam propagation and plasma properties in the neutralizer and the E-RID of the ITER Neutral Beam Injector](#)

A.F. Lifschitz, A. Revel, L. Caillault et al.

# Design of the Prototype Negative Ion Source for Neutral Beam Injector at ASIPP\*

WEI Jianglong (韦江龙), XIE Yahong (谢亚红), LIANG Lizhen (梁立振),  
 GU Yuming (顾玉明), YI Wei (邑伟), LI Jun (李军), HU Chundong (胡纯栋),  
 XIE Yuanlai (谢远来), JIANG Caichao (蒋才超), TAO Ling (陶玲),  
 SHENG Peng (盛鹏), XU Yongjian (许永建)

Institute of Plasma Physics, Chinese Academy of Sciences, Hefei 230031, China

**Abstract** In order to support the design, manufacture and commissioning of the negative-ion-based neutral beam injection (NBI) system for the Chinese Fusion Engineering Test Reactor (CFETR), the Hefei utility negative ion test equipment with RF source (HUNTER) was proposed at ASIPP. A prototype negative ion source will be developed at first. The main bodies of plasma source and accelerator of the prototype negative ion source are similar to that of the ion source for EAST-NBI. But instead of the filament-arc driver, an RF driver is adopted for the prototype negative ion source to fulfill the requirement of long pulse operation. A cesium seeding system and a magnetic filter are added for enhancing the negative ion density near the plasma grid and minimizing co-extracted electrons. Besides, an ITER-like extraction system is applied inside the accelerator, where the negative ion beam is extracted and accelerated up to 50 kV.

**Keywords:** negative ion source, neutral beam injection, CFETR

**PACS:** 29.27.Ac, 52.50.Gj, 52.59.Bi

**DOI:** 10.1088/1009-0630/18/9/13

(Some figures may appear in colour only in the online journal)

## 1 Introduction

A new tokamak device named China Fusion Engineering Test Reactor (CFETR) is under engineering conceptual design<sup>[1,2]</sup>. The major missions of CFETR are:

- a. Demonstration of the fusion energy with a minimum power 50–200 MW;
- b. Long pulse or steady-state operation with duty cycle time  $\geq 0.3$ –0.5;
- c. Demonstration of full cycle of tritium self-sustained with tritium breeding ratio (TBR)  $\geq 1.2$ .

The neutral beam injection (NBI) has been determined as the major method for CFETR plasma heating and current driver. The power proposed target of NBI is 20 MW at 500 keV (potential upgrade to 40 MW), and off-axis injection. At such level of beam energy, the negative-ion-based NBI system is inevitable to attain an acceptable neutralization efficiency. But in China, there is not yet a negative-ion-based NBI system or test facility, and relevant research is little. Therefore, ASIPP is developing Hefei utility negative ion test equipment with RF source (HUNTER) for the crucial techniques of negative-ion-based NBI system facing the future fusion reactor.

Considering the research accumulations and

available experimental conditions at ASIPP, a prototype negative ion source for HUNTER will be developed and tested at first (main parameters are listed in Table 1), as the foundation of giant negative ion source for CFETR (at least half-scaled ITER negative ion source). The research of the prototype negative ion source will be divided into two phases. In the first phase, the negative ions are produced in the cesium-seeded plasma and extracted only, in order to understand and accumulate the basic physics of long-pulse negative ion source. The source plasma performance will be improved with the spectroscopic and probe measurements<sup>[3]</sup>. The target of calorimetric current density is 350 A/m<sup>2</sup> with H<sub>2</sub> gas at extraction voltage of 10 kV, and H<sup>-</sup>/e ratio is expected to be larger than 1. In the second phase, the negative ions are accelerated up to 50 kV due to the limitations of the present HV power supply. However, the beam steering and stripping losses can still be investigated by the beam dump with infrared thermal camera and the Doppler shift spectrometry<sup>[4]</sup>. The ultimate aim is to become a new utility negative ion source for fundamental research, and to have similar beam parameters and role with the BATMAN at IPP-Garching<sup>[5]</sup>, the 10 A negative ion source at JAEA<sup>[6]</sup> and the 1/3 scaled negative ion source at NIFS<sup>[7]</sup>.

\*supported by National Natural Science Foundation of China (Nos. 11505224, 11575240, 11405207), the National Magnetic Confinement Fusion Science Program of China (Nos. 2013GB101001, 2013GB101002, 2013GB101003), International Science and Technology Cooperation Program of China (No. 2014DFG61950), and Foundation of ASIPP (No. DSJJ-14-JC07)

**Table 1.** Main parameters of prototype negative ion source for HUNTER

Parameter	Description
Plasma source	RF driver + bucket chamber
RF driver	50 kW, $\phi 200$ mm
Bucket chamber	650 mm(L) $\times$ 260 mm(W) $\times$ 28 mm(H)
Extraction area	120 mm $\times$ 480 mm
Apertures	5 $\times$ 6 each group, 4 groups, $\phi 14$ mm, spacing 22 mm $\times$ 20 mm
Extractor	<12 kV
Accelerator	Single-stage, <50 kV

The design of the prototype negative ion source is based on that of EAST positive ion sources, which have successfully operated for EAST-NBI system [8–11]. But some crucial elements are redesigned or added for negative ion production, extraction and acceleration. The source plasma is generated in an RF driver to fulfill the requirement of long pulse operation [12] and the original bucket chamber without filaments acts as an expansion region for negative ion production. A Cs supply system and an external magnetic filter are added to enhance the negative ion beam current and suppress the co-extracted electrons [13,14]. The negative ions are extracted and accelerated through a new multi-aperture grid system, which is also different from the original multi-slot grid system. The paper concentrates on the design of the plasma source and the grid system.

## 2 Plasma source

The RF-driven plasma source concept originates from ITER design [15–17] and has been demonstrated in several test facilities at IPP-Garching (BATMAN, MANITU, RADI, ELISE) [18,19]. Fig. 1 shows the details of the prototype negative ion source with the inductively coupled plasma discharge. A cylindrical driver with external RF antenna is attached to the driver plate of a bucket chamber, where the source plasma is generated and expands to the extraction region near the plasma grid. Such configuration can be easily improved to larger input power and more homogenous plasma profile by combining two similar cylindrical drivers. Cs is delivered from an oven connected to the driver plate.

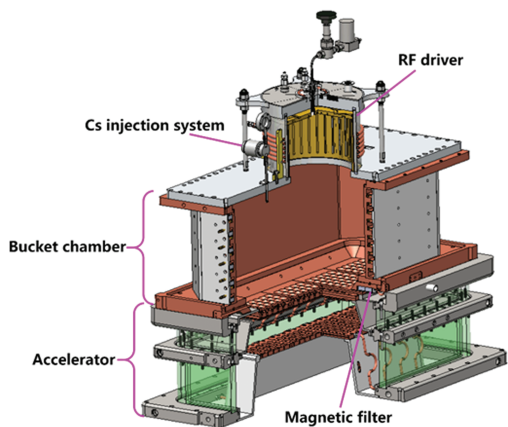


**Fig.1** The prototype negative ion source for HUNTER at ASIPP

### 2.1 RF driver

The driver design is based on the RF driven prototype source for ITER [20]. The driver is a cylinder including a lateral wall in quartz and a back cover in aluminum, as shown in Fig. 2, where the RF power is transferred into and the plasma is generated. The inner diameter of the quartz cylinder is 209 mm, the height is 120 mm, and the thickness is 9 mm. The quartz cylinder directly contacts the driver back cover and the driver plate of the bucket chamber with two O-rings, for vacuum maintenance and mechanical protection. The driver back cover is supported by four rods from the driver plate. The working gas inlet is positioned in the center of the driver back cover, and two water feedthroughs nearby connect to Faraday shield. A startup filament is used to supply the initial electrons to ignite the plasma. A checkerboard multi-cusp field is formed with a pattern of permanent magnets embedded in the driver back cover.

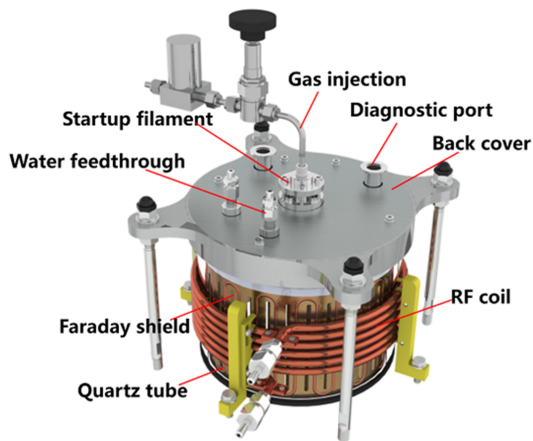


**Fig.2** Design of the RF driver

The RF coil wound around the driver cylinder is made out of a copper tube, where the cooling water flows to remove the heat generated by the current. The outer diameter of the tube is 6.5 mm and the inner diameter is 4 mm. The number of windings is six and the adjacent windings are properly separated by four insulated fixtures. A larger PTFE tube covers the outside of the coil for further insulation.

The actively cooled Faraday shield is a copper cylinder with a back plate, which is inserted between the plasma and quartz cylinder, in order to protect against the erosion and thermal radiation. The Faraday shield is 4 mm in thickness, 200 mm in diameter and

120 mm in height, as shown in Fig. 3. Thirty-two slits are cut on its lateral wall to allow the inductive field to penetrate through, and the direction of each slit is rotated 45 degrees against the radial direction. There is a cooling channel embedded between each two adjacent slits, and each four cooling channels are supplied in a series from the water inlet and outlet network of channels on different levels of the back plate. Either inlet or outlet network of channels confluent to an outside water feed through.

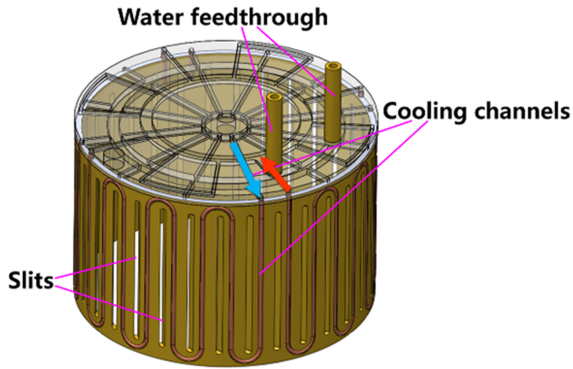


**Fig.3** Design of the Faraday shield, the blue arrow means water inlet and the red arrow means water outlet

## 2.2 Bucket chamber

The design and manufacture of the bucket chamber has been operated successfully for the sources of EAST-NBI system [21], and its main function is to form a vacuum space for gas discharge. The planar lateral wall is 8 mm thick, in order to equalize the source weight and deformation limitation. Five rows of stiffening ribs are attached and supported around the outside of the planar lateral wall, and each stiffening rib is embedded in a cooling water circle. The whole bucket chamber is made out of copper, which benefits the uniformity and conduction of local heat loads on the internal surface towards the cooling channels. The requirement of Cs recycling in the negative ion source makes more demands of temperature control on the lateral wall than that in the positive ion source because either hot spots (above 70 °C) or cold spots (under 40 °C) are detrimental of the cesium behavior [22,23].

The bucket chamber is closed at its rear end by the driver plate. The driver plate has inertia cooling to remove the heat load from the plasma and back streaming positive ions, though the acceleration voltage is not so high. The cooling tubes are welded in the grooves on the outside of the plate. The driver plate has two injection holes for Cs vapor, but only one will be used. The Cs supply system mainly comprises Cs oven, valve, and connecting tube [24]. The quantity of injected Cs is controlled by the oven temperature (150 °C–250 °C).

The source plasma is confined by the line-cusp magnetic field generated with Sm-Co permanent magnets, which are attached between the stiffening

ribs on the outside of the lateral wall and in the special grooves on the outside of the driver plate. These magnets are covered by several soft iron plates. The cusp magnetic strength is 2500 Gs on the inner chamber surface. An additional two pairs of magnets are embedded on the bottom of the chamber in the longitudinal direction, creating a uniform filter field in front of the plasma grid. The filter field along the center line of the chamber is shown in Fig. 4.

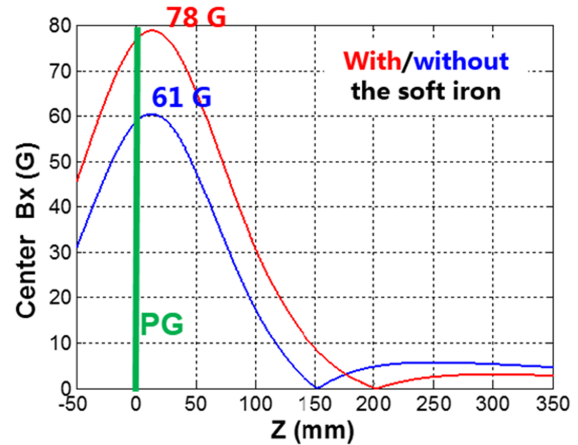


**Fig.4** The value of the filter field along the center line of the chamber with/without soft iron plate outside

## 3 Negative ion accelerator

The negative ion accelerator is a single-stage acceleration system and mainly consists of three grids: plasma grid (PG), extraction grid (EG), and ground grid (GG). Each grid is made out of copper and divided into four identical segments. However, in the first research phase, only the middle two groups of segments will be used for extraction to match the single RF driver. Each segment consists of 6×5 apertures. The aperture spacing is 22 mm×20 mm. The aperture geometry of all grids is indicated in Fig. 5. The first gap (PG-EG) and the second gap (EG-GG) are used for beam extraction and acceleration, respectively. A molybdenum-made grid (electron suppression grid, ESG) is attached to the EG at the same electric potential, in order to suppress the secondary electrons leakage and steer the negative ion beam [25].

An existing insulator structure for EAST ion source [26] with four supporting flanges and three insulators will be used temporarily to test the extraction of the negative ions. All grids are installed on the matching grid holders. The PG and EG holder are mounted on the first and second supporting flange, respectively. The cooling water circulations of this insulator structure are designed to remove heat load only. But the PG temperature in the negative ion source should increase quickly and be maintained at around 200 °C to optimize the production of the negative ions. Thus, a new insulator structure is under design, which is not within the scope of this paper.



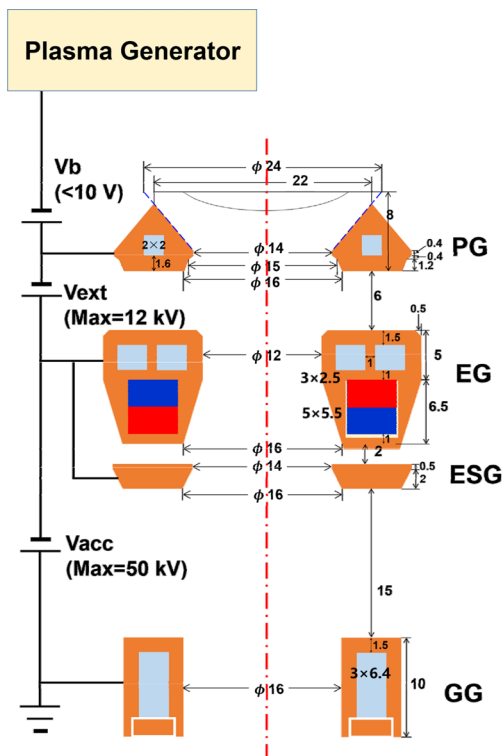


**Fig.5** The aperture geometry of the grid for negative ion accelerator. “ $V_b$ ” represents the biasing voltage between the plasma source and plasma grid, “ $V_{ext}$ ” represents the extraction voltage, and “ $V_{acc}$ ” represents the acceleration voltage

### 3.1 Plasma grid

The aperture geometry of PG is the same as the ITER design [27]. The chamfer design on the plasma side can enhance negative ion current, by increasing the Cs covered area for the surface production and the extraction probability of generated negative ions.

The cooling scheme inside the PG is revealed in Fig. 6. The two inlets and two outlets follow the initial design. The small channels between each aperture row connect these inlets and outlets through two large sinks. The most critical issue for the PG cooling scheme is that the PG should be operated at temperatures around 200 °C. Therefore, the cooling channels with 2 mm×2 mm cross section should sustain a water pressure up to 2 MPa in order to acquire a higher boiling temperature.

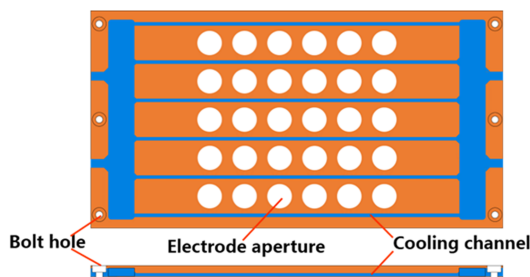


**Fig.6** The cooling scheme of the plasma grid (top and side view)

The plasma grid is positively biased against the source. The bias voltage may draw the negatively charged particles onto the PG surface instead of through the apertures. Due to the large mass ratio between negative ions and electrons, the drop of co-extracted electron current is much more [18]. Thus, the bias voltage can contribute to the suppression of the co-extracted electrons.

### 3.2 Extraction grid

The major function of the extraction grid is deflecting co-extracted electrons onto its surface. Rows of permanent magnets are embedded in the EG to filter the co-extracted electrons out of the beam. Many experimental and simulation results showed that the impact positions of most deflected electrons concentrate as a curve or some points on the top surface of EG [28–30]. In order to remove power load effectively, an ITER-like extraction grid is adopted, where the cooling channels locate near the top surface, as shown in Fig. 7. Two separated cooling channels are placed between aperture rows. Such pair of cooling channels are 3 mm wide and 2.5 mm deep, and 1 mm apart. This design has a better heat exchange performance than that of the single large channel [27]. These small cooling channels also connect two inlets and two outlets through two large sinks.

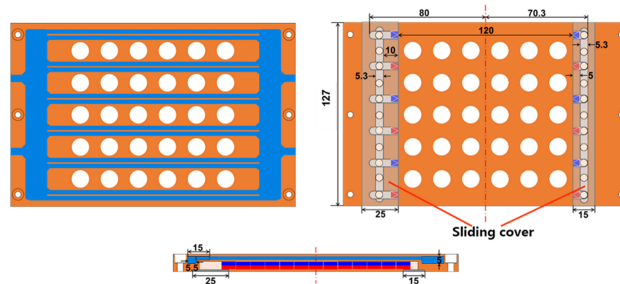


**Fig.7** The cooling scheme and magnet arrangement of extraction grid (top, back and side view)

The electron suppression magnet rows just lie downward of the cooling channels. The size of magnet (5 mm wide and 5.5 mm deep) is selected to be as large as possible without a big influence of the EG structure. The magnets can be inserted from one side through a window opening on the back side, which will be closed by the sliding covers. The strengths of the transverse magnetic field along the aperture centerline are shown in Fig. 8. The maximum strength is about 500 Gs at the EG entrance and the strength at the PG entrance is about 140 Gs, which could influence co-extracted electron current. The distribution of the maximum strength is indicated in Fig. 9. The lower strength along the edge aperture row is inevitable but acceptable.

### 3.3 Ground grid

The power load on the GG is estimated to be 10%–20% of the total power, according to the experimental

results of single-stage accelerator of LHD-NBI [31]. The cooling scheme is similar to the PG scheme with the larger cooling channels (3 mm wide and 6 mm deep). A multi-slot GG is in development based on the successful technique and experience of EAST-NBI accelerator, in order to reduce the power load and breakdown on the GG.

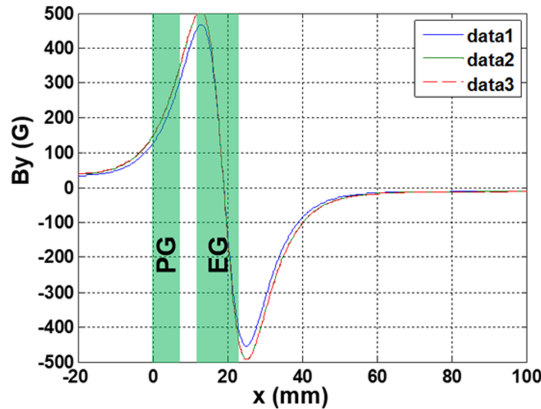


**Fig.8** The strengths of the transverse magnetic field along the three different apertures centerline: data 1 along the edge aperture, data 3 along the middle aperture and data 2 between them

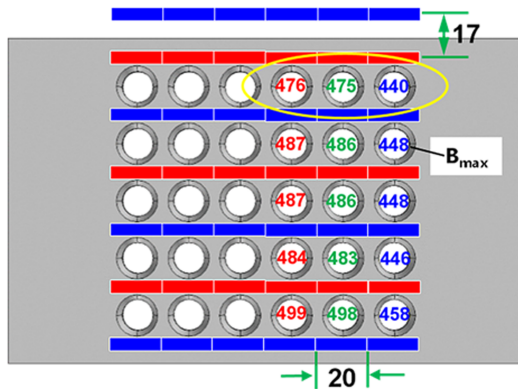


**Fig.9** The distribution of the maximum strength in different apertures

## 4 Conclusion

The Hefei utility negative ion test equipment with Rf source (HUNTER) at ASIPP will be a very important step towards the CFETR neutral beam injector. It will complete the domestic research on negative-ion-based NBI system, and will help to gain the experience on design and operation of negative ion source.

The prototype negative ion source for HUNTER has been designed with some additions and modifications on the EAST positive ion source, according to the operating negative ion sources. It consists of an RF-driven plasma source and negative ion accelerator with multi-aperture grids. A Cs supply system and an external magnetic filter are added to enhance the negative ion beam current and suppress the co-extracted electrons. Most of the negative ions are

produced on the Cs covered layer of plasma grid and extracted by the extraction grid. The co-extracted electrons are wiped out by the magnets embedded inside the extraction grid. Finally,  $H^-$  negative beam of  $350 A/m^2$  is expected to be extracted and accelerated up to 50 kV, and  $H^-/e$  ratio is required to be larger than 1.

It is planned to manufacture and assemble the source and test bed within the first year, and start the experiment in the next year.

## Acknowledgment

The authors are much indebted to the other members of EAST NBI group for their continuous encouragement and support.

## References

- 1 Wan B N, Ding S Y, Qian J P, et al. 2014, IEEE Transactions on Plasma Science, 42: 495
- 2 Song Y T, Wu S T, Li J G, et al. 2014, IEEE Transactions on Plasma Science, 42: 503
- 3 Xie Y H, Hu C D, Liu S, et al. 2012, Review of Scientific Instruments, 83: 013301
- 4 Liang L Z, Wang Y, Zhao X X, et al. 2015, Physica Scripta, 90: 045603
- 5 Speth E, Falter H D, Franzen P, et al. 2006, Nuclear Fusion, 46: S220
- 6 Hanada M, Seki T, Takado N, et al. 2006, Nuclear Fusion, 46: S318
- 7 Ikeda K, Nakano H, Tsumori K, et al. 2013, New Journal of Physics, 15: 103026
- 8 Hu C D, Xie Y H, Xie Y L, et al. 2016, Review of Scientific Instruments, 87: 02B301
- 9 Hu C D, Xie Y H, Xie Y L, et al. 2015, Plasma Science and Technology, 17: 817
- 10 Hu C D. 2015, Plasma Science and Technology, 17: 1
- 11 Xie Y H, Hu C D, Liu S, et al. 2014, Review of Scientific Instruments, 85: 02B315
- 12 Franzen P, Fantz U. 2014, Fusion Engineering and Design, 89: 2594
- 13 Schiesko L, McNeely P, Fantz U, et al. 2011, Plasma Physics and Controlled Fusion, 53: 085029
- 14 Fantz U, Schiesko L, Wunderlich D. 2014, Plasma Sources Science and Technology, 23: 044002
- 15 Marcuzzi D, Agostinetti P, Dalla Palma M, et al. 2010, Fusion Engineering and Design, 85: 1792
- 16 Marcuzzi D, Dalla Palma M, Pavei M, et al. 2009, Fusion Engineering and Design, 84: 1253
- 17 Sonato P, Agostinetti P, Anaclerio G, et al. 2009, Fusion Engineering and Design, 84: 269
- 18 Franzen P, Falter H D, Fantz U, et al. 2007, Nuclear Fusion, 47: 264
- 19 Franzen P, Fantz U, Wunderlich D, et al. 2015, Nuclear Fusion, 55: 053005
- 20 Xie Y H, Hu C D, Jiang C C, et al. 2016, Review of Scientific Instruments, 87: 02B302
- 21 Hu C D, NBI Team. 2012, Plasma Science and Technology, 14: 567

- 22 Fantz U, Franzen P, Kraus W, et al. 2009, Nuclear Fusion, 49: 125007
- 23 Kojima A, Hanada M, Yoshida M, et al. 2015, AIP Conference Proceedings, 1655: 06002
- 24 Rizzolo A, Pavei M, Pomaro N. 2013, Fusion Engineering and Design, 88: 1007
- 25 Takeiri Y. 2010, Review of Scientific Instruments, 81: 02B114
- 26 Wei J L, Li J, Hu C D, et al. 2014, Review of Scientific Instruments, 85: 073504
- 27 de Esch H P L, Kashiwagi M, Inoue T, et al. 2013, AIP Conference Proceedings, 1515: 512
- 28 Nocentini R, Gutser R, Heinemann B, et al. 2011, Fusion Engineering and Design, 86: 916
- 29 Kashiwagi M, Umeda N, Tobari H, et al. 2014, Review of Scientific Instruments, 85: 02B320
- 30 Agostinetti P, Antoni V, Cavenago M, et al. 2011, Nuclear Fusion, 51: 063004
- 31 Takeiri Y, Kaneko O, Tsumori K, et al. 2006, Nuclear Fusion, 46: S199
- (Manuscript received 11 September 2015)  
(Manuscript accepted 12 January 2016)  
E-mail address of corresponding author LIANG Lizhen:  
lzliang@ipp.ac.cn